The Phase Diagram of High Temperature QCD with Three Flavors of Improved Staggered Quarks

The MILC Collaboration: C. Bernard, T. Burch, T. DeGrand, C. DeTar, Steven Gottlieb, E. Gregory, J. Hetrick, U.M. Heller, R. Sugar, and D. Toussaint

I. Introduction

We are carrying out a study of high temperature QCD with three flavors of improved staggered quarks [1] using a one–loop Symanzik improved gauge action [2] and the Asqtad quark action [3]. Both the gauge and quark actions have all lattice artifacts removed through order a^2 at tree level, and are tadpole improved. (a is the lattice spacing). Thus, the leading order finite lattice spacing artifacts are of order $\alpha_s a^2$, a^4. We are considering two cases: 1) all three quarks have the same mass, m_q; and 2) the two lightest mass quarks have equal mass, $m_{u,d}$, and the mass of the third quark is fixed at that of the strange quark, m_s. We refer to these cases as $N_f = 3$ and $N_f = 2+1$, respectively.

The Asqtad action has a significantly better dispersion relation for the quarks than the standard Kogut–Susskind and Wilson quark actions [4], which helps decrease lattice artifacts in the energy and pressure, as can be seen in Figures 1 and 2. The Asqtad action also exhibits excellent scaling properties in the lattice spacing [5]. This is illustrated in Figure 3, where we plot the mass of the rho meson versus the square of the lattice spacing in the quenched approximation for the conventional Kogut–Susskind, Clover–Wilson and Asqtad actions. Here, and elsewhere in this poster, we determine the lattice spacing from the the static $\bar{Q}Q$ potential, and express dimensionful quantities in terms of r_1 defined by $r_1^2 F_{\bar{Q}Q}(r_1) = 1$, which leads to $r_1 \approx 0.35$ fm. Finally, the Asqtad action has better flavor symmetry properties than the conventional Kogut–Susskind action [4], although not as good as the HYP action [6]. In Figure 4, we plot the mass of the second lightest pion in units of r_1 as a function of a^2, for fixed lowest pion mass, which is shown as a horizontal blue line. We estimate that for lattices with eight to ten time slices, the kaon will be heavier than the heaviest non-Goldstone pion in the neighborhood of the finite temperature transition or crossover.

We have attempted to vary the temperature while keeping all other physical quantities constant. To this end we have performed a set of spectrum calculations at $a = 0.13$ fm and 0.20 fm for three equal mass quarks. (The lattice spacing is determined from the static $\bar{Q}Q$ potential). We determine m_s from the requirement that $m_{\eta_{ss}}/m_\phi \approx 0.673$. We have performed spectrum calculations at both lattices spacings with $m_q = m_s$, $0.6m_s$ and $0.4m_s$, with an additional calculation at $0.2m_s$ in progress. We would like to carry out our thermodynamics studies with three equal mass quarks for $m_{\eta_{ss}}/m_\phi$ fixed, but this quantity will, of course, vary slightly with lattice spacing if we keep m_q/m_s fixed. So, at $a = 0.2$ fm we perform linear interpolations of $m^2_{\eta_{ss}}$ and m_ϕ in the quark mass to determine the precise values of m_q for which $m_{\eta_{ss}}/m_\phi$ will take on the values found at $a = 0.13$ fm. Then to determine the values of am_q and a for thermodynamics studies studies with 0.13 fm $< a <$ 0.20 fm, we perform linear interpolations of the logarithms of these quantities in the gauge coupling, $10/g^2$.

Our approach for thermodynamics studies with $m_{u,d} < m_s$ is quite similar. In this case we wish to vary the temperature keeping both m_π/m_ρ and $m_{\eta_{ss}}/m_\phi$ fixed. We have therefore performed a set of spectrum calculations at $a = 0.13$ fm and 0.20 fm with the mass of the light quarks, $m_{u,d} = 0.6m_s$, $0.4m_s$ and $0.2m_s$. An additional spectrum calculation with $m_{u,d} = 0.1m_s$ is in progress. In these calculations the mass of the heavy quark is fixed at m_s, as determined from spectrum calculations with three equal mass quarks. In our spectrum runs at $a = 0.13$ fm [4] we found that $m_{\eta_{ss}}$ varied by less than 2% and m_ϕ by less than 1% for $0.2m_s \leq m_{u,d} \leq m_s$ and the heavy quark mass held fixed at m_s. So, the neglect of the dependence of $m_{\eta_{ss}}$ and m_ϕ on $m_{u,d}$ is well justified. In these studies we performed linear interpolations of m^2_π and m_ρ at $a = 0.20$ fm to determine the values of $m_{u,d}$ for which m_π/m_ρ takes on the values found at $a = 0.13$ fm. Then for 0.13 fm $< a <$ 0.20 fm we perform linear interpolations of the logarithms of a, am_s, and $am_{u,d}$ in the gauge coupling along lines of constant m_π/m_ρ and $m_{\eta_{ss}}/m_\phi$.

II. Results for $\mathbf{N_f = 3}$

For three equal mass quarks, $N_f = 3$, we have carried out thermodynamics studies on lattices with four, six and eight times slices, and aspect ration $N_s/N_t = 2$, Here N_s and N_t are the spatial and temporal dimensions of the lattice in units of the lattice spacing. The spectrum calculations and interpolations described above allowed us to determine the values of the quark mass, m_q, that keep $m_{\eta_{ss}}/m_\phi$ fixed as the gauge coupling is varied. They also enabled us to determine the value of the lattice spacing, and therefore the temperature for each run.

In Figure 5 we plot the real part of the Polyakov loop as a function of temperature on $16^3 \times 8$ lattices. In this figure, as elsewhere, we give the values of m_q/m_s for $a = 0.13$ fm. The corresponding values of $m_{\eta_{ss}}/m_\phi$ are given in Table 1. The Polyakov loop shows a crossover from confined behavior at low temperature to deconfined behavior at high temperature, but the transition is not particularly sharp. The insensitivity of the Polyakov loop to the quark mass at fixed temperature or lattice spacing is, perhaps, not surprising. We have determined the lattice spacing from the heavy quark potential, and in our spectrum runs we adjusted the coupling constant to keep the lattice spacing fixed as the quark mass is varied. Since the Polyakov loop, like the heavy quark potential, is determined from measurements of purely gluonic operators, our procedure is likely to minimize the dependence of the Polyakov loop on the quark mass.

$N_f = 3$		$N_f = 2+1$	
m_q/m_s	$m_{\eta_{ss}}/m_\phi$	$m_{u,d}/m_s$	m_π/m_ρ
1.0	0.673	0.6	0.582
0.6	0.583	0.4	0.509
0.4	0.504	0.2	0.392

Table 1: In the first column we show the value of m_q/m_s at lattice spacing 0.13 fm, which produced the $m_{\eta_{ss}}/m_\phi$ ratio shown in the second column for spectrum calculations with three equal mass quarks. In the third column we give the value of $m_{u,d}/m_s$ which produced the m_π/m_ρ ratio shown in the fourth column for spectrum calculations with two equal mass light quarks, and the mass of the heavy quark fixed at m_s.

The number of conjugate gradient iterations needed to obtain a given accuracy for the calculation of the quark propagator gives an indication of the change in physics as the temperature is varied. We show this quantity in Figure 6 for the three values of the quark mass we have studied on $16^3 \times 8$ lattices. The sharpening of the crossover as the quark mass is reduced is evident. A more physical signal for the crossover is given by the quark number susceptibility. In Figure 7 we show the triplet susceptibility for the three quark masses we have studied on $12^3 \times 6$ lattices, and in Figure 8 we illustrate the dependence of this quantity on lattice spacing by plotting results at fixed quark mass for three values of N_t. The solid lines on the right of these figures indicate the values of the susceptibility for free quarks in the continuum (black line) and on the finite lattices on which the simulations took place (colored lines). The close agreement between the $N_t = 6$ and 8 results is an indication of the excellent scaling properties in lattice spacing of the Asqtad action. All of these results are indicative of a crossover, rather than a bona fide phase transition. This result is consistent with earlier studies which found phase transitions only for smaller values of the quark mass than we have studied to date.

In Figures 9 and 10 we show the chiral order parameter, $\bar{\psi}\psi$ as a function of temperature for $m_q = m_s$, $0.6m_s$ and $0.4m_s$ on $12^3 \times 6$ and $16^3 \times 8$ lattices, respectively. The black bursts in these figures are linear extrapolations of $\bar{\psi}\psi$ in the quark mass to $m_q = 0$ for fixed temperature. These figures indicate that for $m_q = 0$ there is no phase transition below approximately 180 MeV.

III. Results for $\mathbf{N_f = 2+1}$

The $N_f = 2+1$ thermodynamics studies were carried out on $12^3 \times 6$ and $16^3 \times 8$ lattices. In this phase of our work we performed simulations with two degenerate light quarks and the heavy quark mass held equal to that of the strange quark. The spectrum calculations and interpolations described above allowed us to determine the values of the heavy and light quark masses needed to keep m_π/m_ρ and $m_{\eta_{ss}}/m_\phi$ fixed as the gauge coupling was varied. They also allowed us to determine the lattice spacing, and therefore the temperature for each run.

In Figure 11 we plot the real part of the Polyakov loop as a function of temperature on $16^3 \times 8$ lattices for the three values of $m_{u,d}$ studied to date. As in the $N_f = 3$, study we observe a crossover from confined to deconfined behavior, rather than a sharp transition, and little dependence on the light quark mass. In Figure 12 we show the number of conjugate gradient iterations needed for inversion of the Dirac operator for the light quarks on $16^3 \times 8$ lattices. In this case there is a clear sharpening of the crossover as the light quark mass is reduced. In Figure 13 we plot the triplet quark number susceptibility for the light quarks for the three values of $m_{u,d}$ we have studied on $16^3 \times 8$ lattices. In Figure 14 we show this quantity for $m_{u,d} = 0.2m_s$ on both $12^3 \times 6$ and $16^3 \times 8$ lattices. The close agreement between the $N_t = 6$ and 8 results again illustrates the excellent scaling properties of the action. As in the case of $N_f = 3$, all of these results are indicative of a crossover, rather than a bona fide phase transition.

In Figures 15 and 16 we plot the chiral order parameter as a function of temperature on $12^3 \times 6$ and $16^3 \times 8$ lattices. The green, blue and red plotting symbols are data for $m_{u,d} = 0.6m_s$, $0.4m_s$ and $0.2m_s$ respectively, and the black bursts are linear extrapolations in $m_{u,d}$ for fixed temperatures. These figures suggest that there is no phase transition for $m_{u,d} = 0$, and the heavy quark mass equal to that of the strange quark, for $T < 170$ MeV. Whether there is a transition at higher temperature, and the nature of such a transition, if it does exist, will require simulations at smaller values of $m_{u,d}$, which we plan to carry out during the coming year.

This work was supported by the U.S. Department of Energy and National Science Foundation. It used computing resources at Florida State University (SP), FNAL, NERSC, NPACI, and the University of Utah (CHPC).

References

[1] Earlier reports on this work can be found in The MILC Collaboration, C. Bernard, *et al.*, Nucl. Phys. (Proc. Suppl.) **106**, 429, (2002); Nucl. Phys. **A702**, 140, (2002).

[2] K. Symanzik, in "Recent Developments in Gauge Theories", eds. G. 't Hooft *et al.*, 313 (Plenum, New York, 1980).

[3] G.P. Lepage, Phys. Rev. D **59**, 074501, (1999); Kostas Orginos, Doug Toussaint and R.L. Sugar, Phys. Rev. D **60**, 054503, (1999).

[4] The MILC Collaboration, C. Bernard, *et al.*, Phys. Rev. D **64**, 054506 (2001).

[5] The MILC Collaboration, C. Bernard, *et al.*, Phys. Rev. D **61**, 111502 (2000).

[6] F. Knechtli and A. Hasenfratz, Phys. Rev. D **63**, 114502, (2001).

[7] F. Karsch, E. Laermann and A. Peikert, Nucl. Phys. **B605**, 579, (2001).

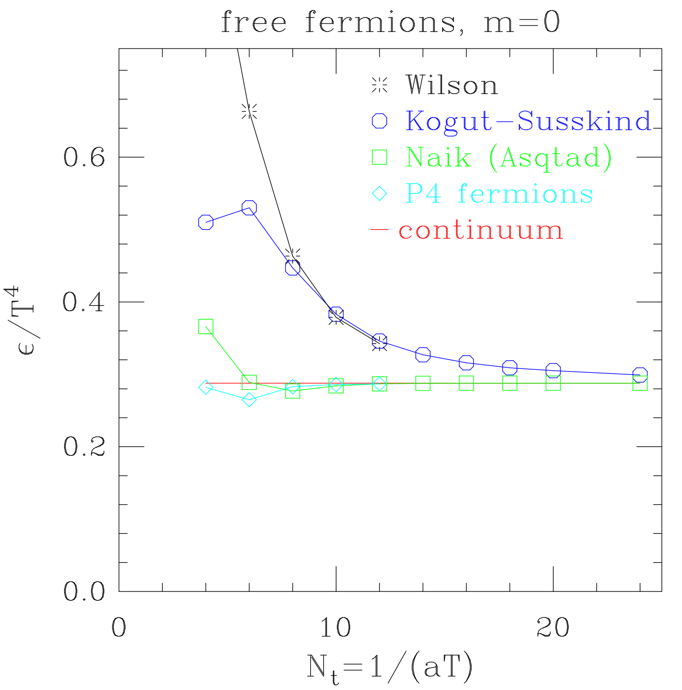

Figure 1: The energy density for free, massless quarks as a function of the temporal lattice size, N_t. For free fermions the Asqtad action reduces to the Naik action. The $P4$ action is the improved staggered fermion action studied by the Bielefeld group [7].

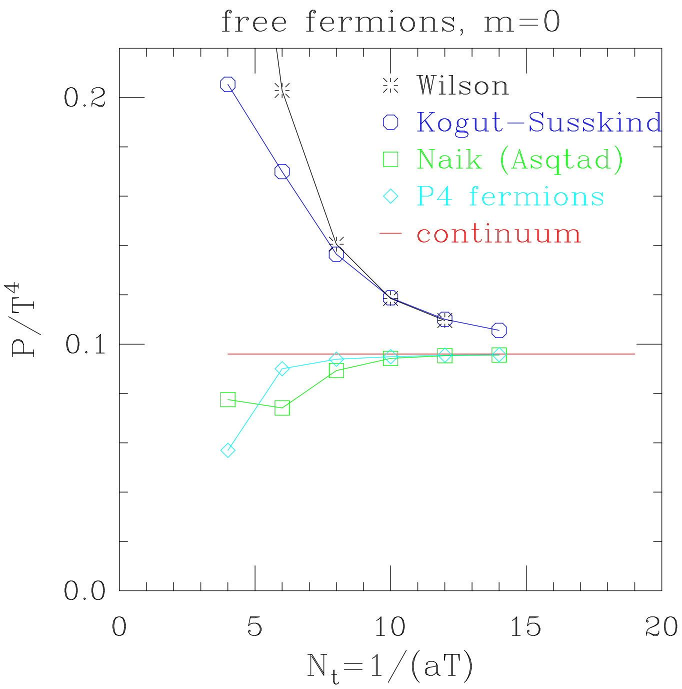

Figure 2: The pressure for free, massless quarks as a function of the temporal lattice size, N_t.

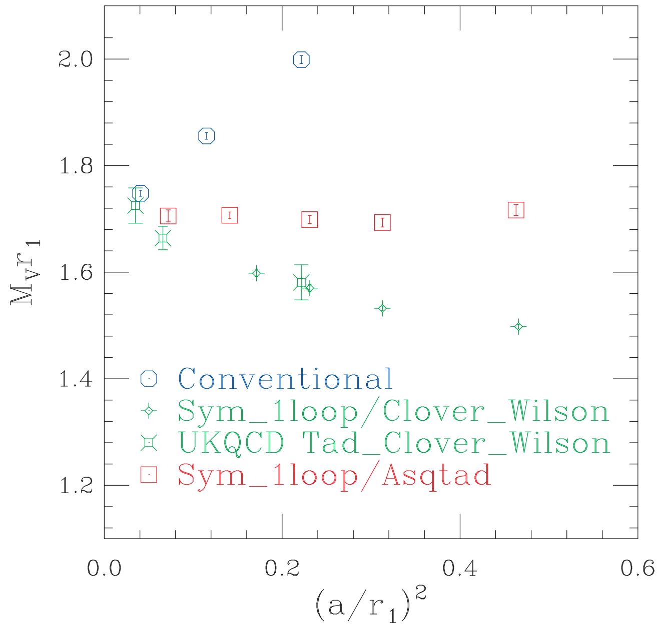

Figure 3: The mass of the rho meson as a function of the square of the lattice spacing in the quenched approximation for the conventional Kogut–Susskind, clover_Wilson and Asqtad actions.

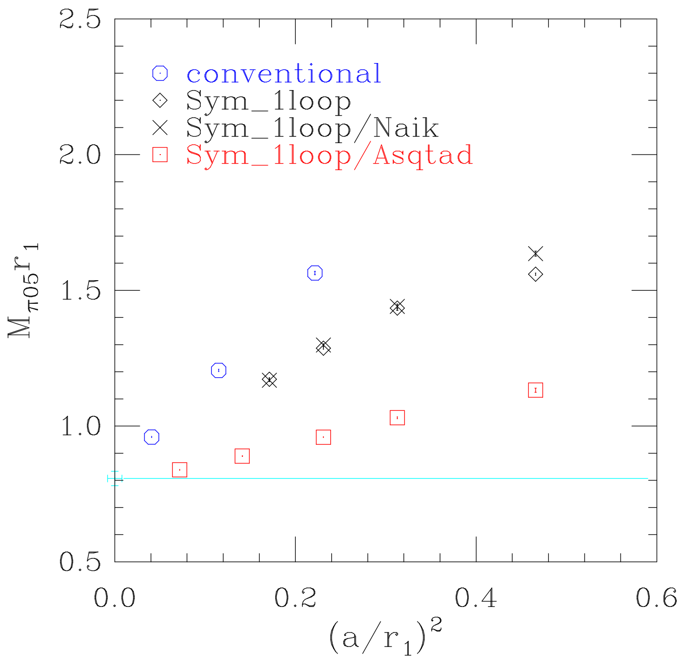

Figure 4: The mass of the second lightest pion in units of r_1, for fixed lowest pion mass shown as the horizontal line, as a function of the square of lattice spacing.

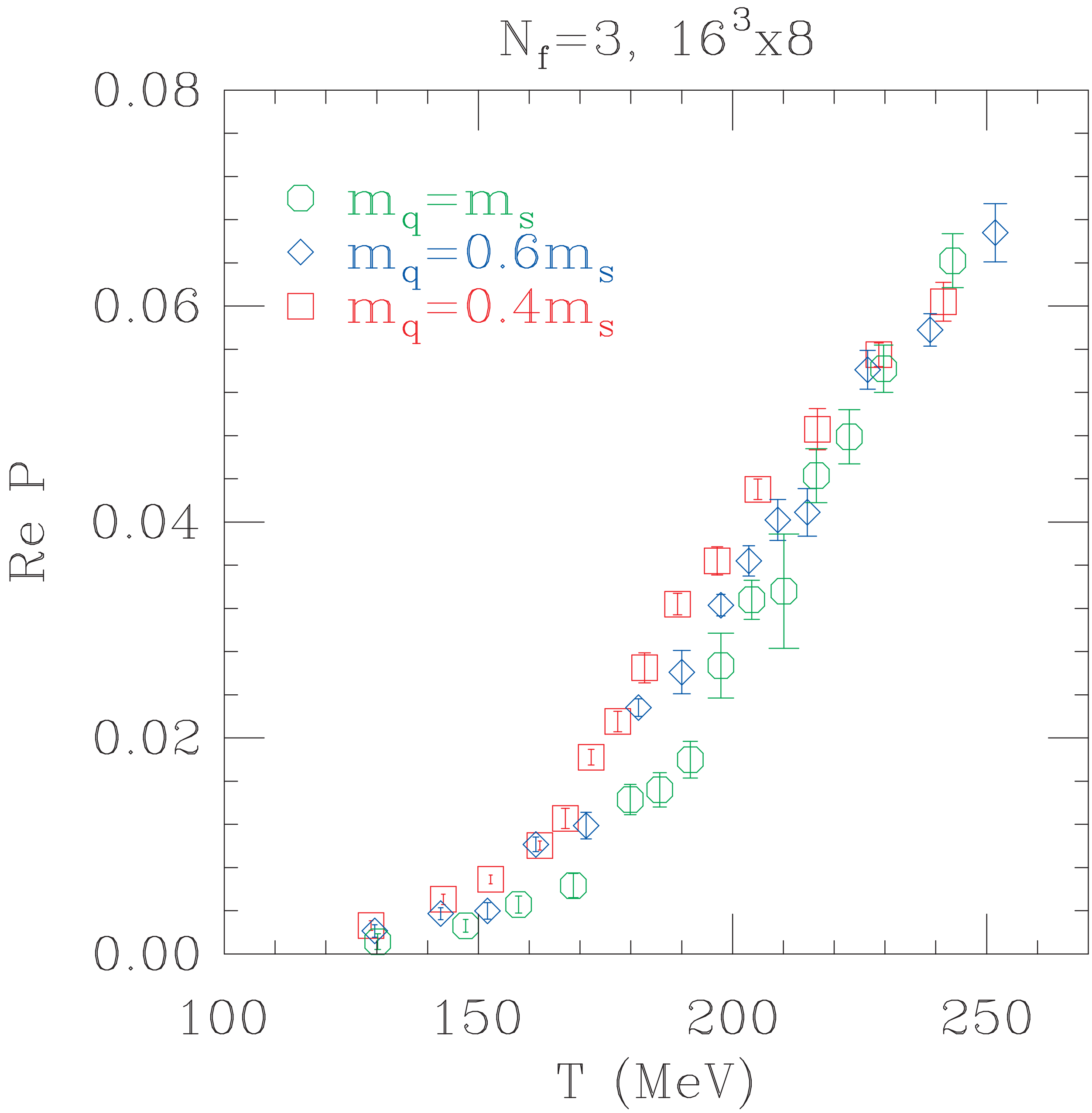

Figure 5: The real part of the Polyakov loop on $16^3 \times 8$ lattices for three degenerate flavors of quarks with masses $m_q = m_s$, $0.6m_s$ and $0.4m_s$.

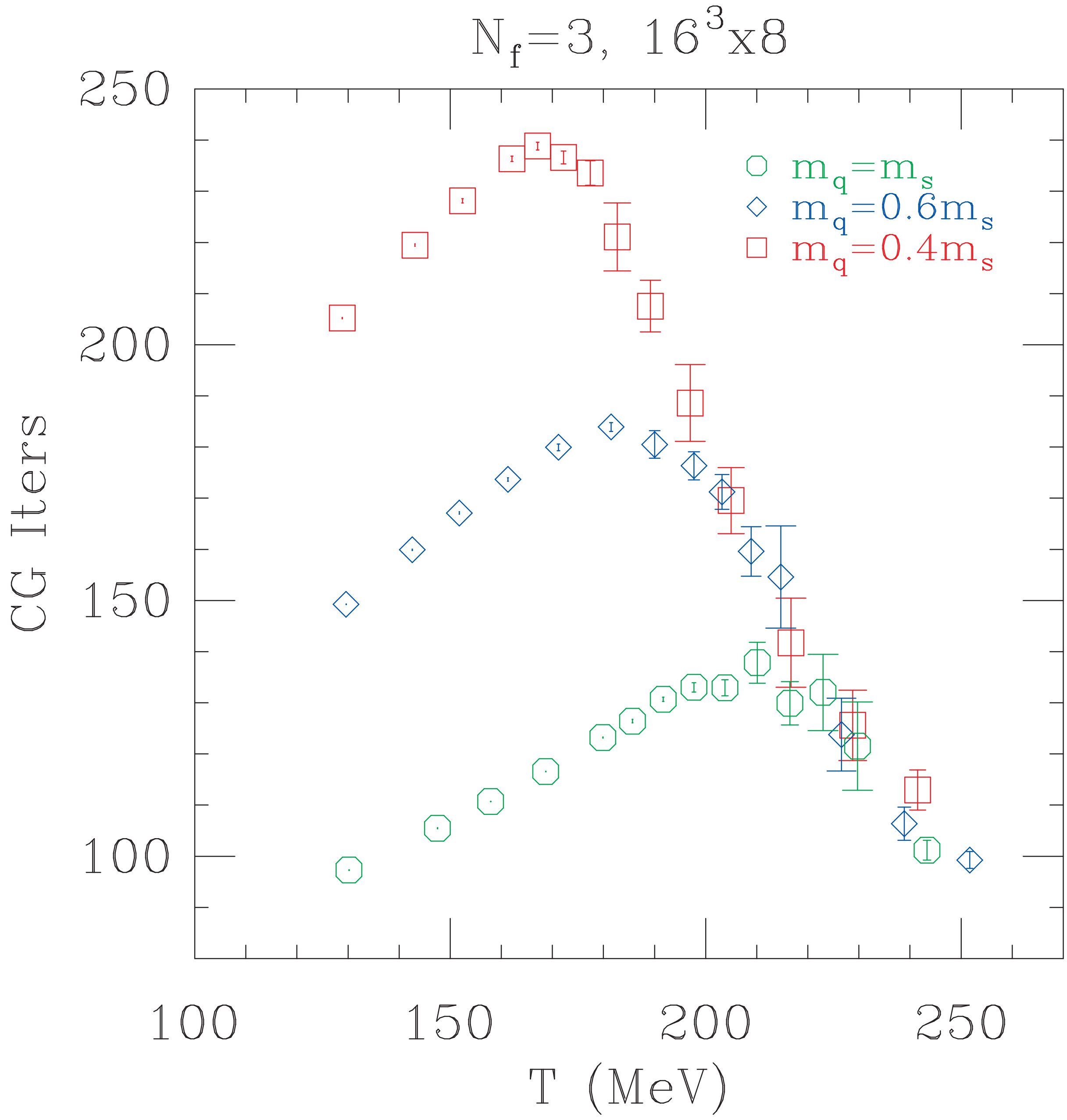

Figure 6: The number of conjugate gradient iterations required for convergence of the inversion of the Dirac operator for three degenerate flavors of quarks with masses $m_q = m_s$, $0.6m_s$ and $0.4m_s$ on $16^3 \times 8$ lattices.

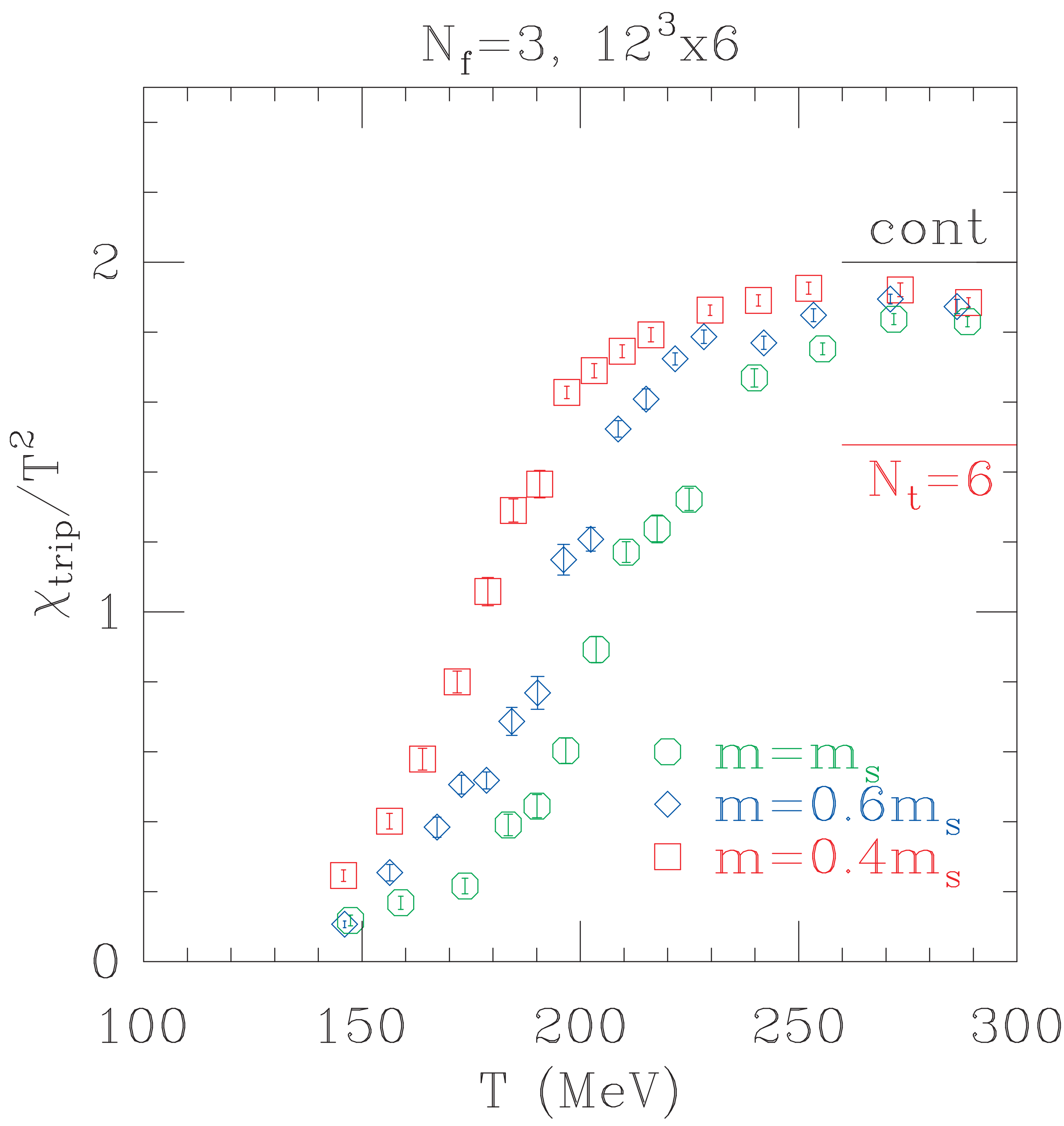

Figure 7: The triplet quark number susceptibility for three degenerate flavors of quarks with masses $m_q = m_s$, $0.6m_s$ and $0.4m_s$ on $12^3 \times 6$ lattices. The black line on the right of the figure indicates the free quark value in the continuum, and the red line the free quark value on a $12^3 \times 6$ lattice.

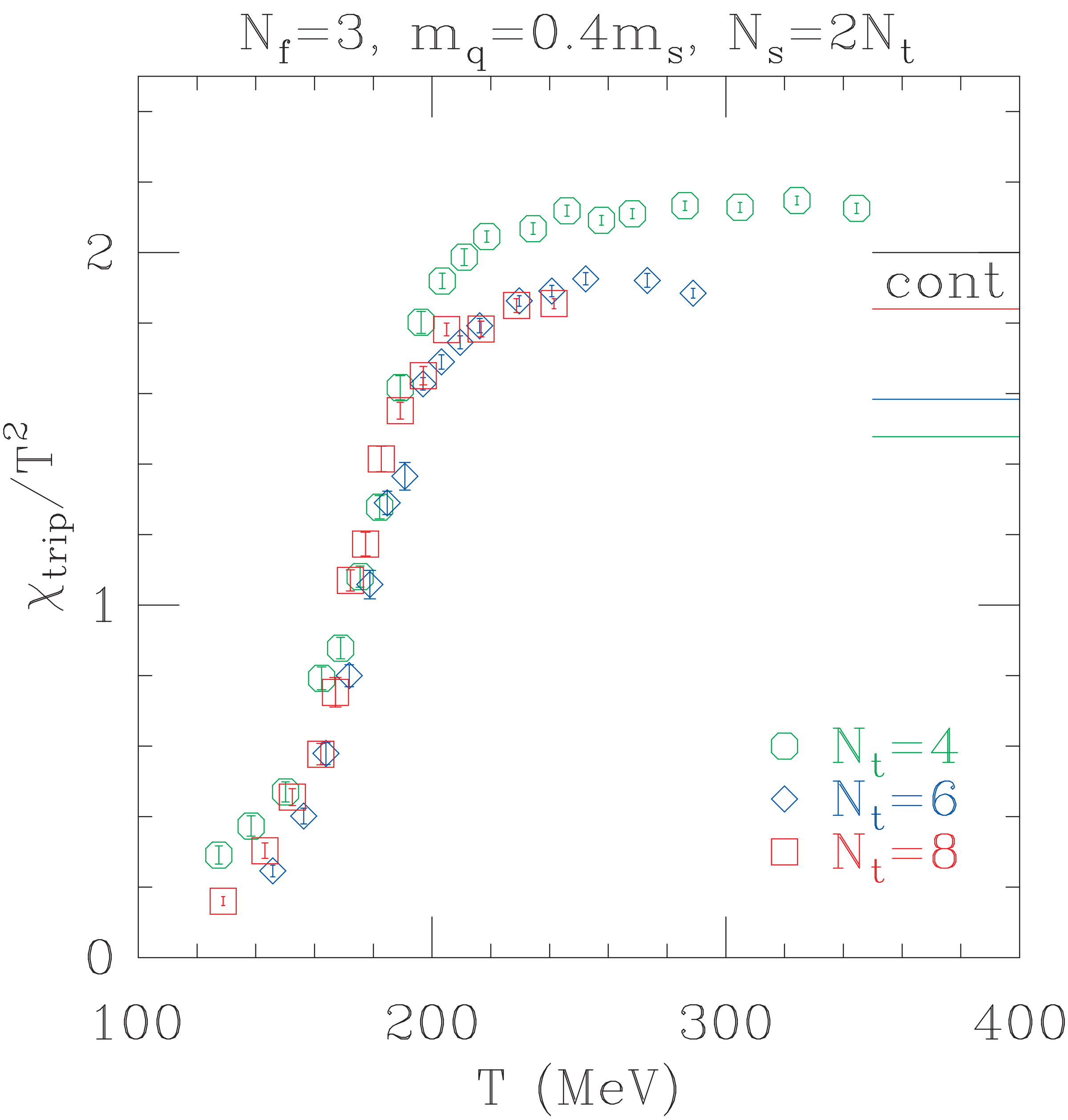

Figure 8: The triplet quark number susceptibility for three degenerate flavors of quarks with mass $m_q = 0.4 m_s$, on $8^3 \times 4$, $12^3 \times 6$ and $16^3 \times 8$ lattices. The black line on the right of the figure indicates the value for free quarks in the continuum, and the colored lines the value for free quarks on the finite lattices on which the simulations were carried out.

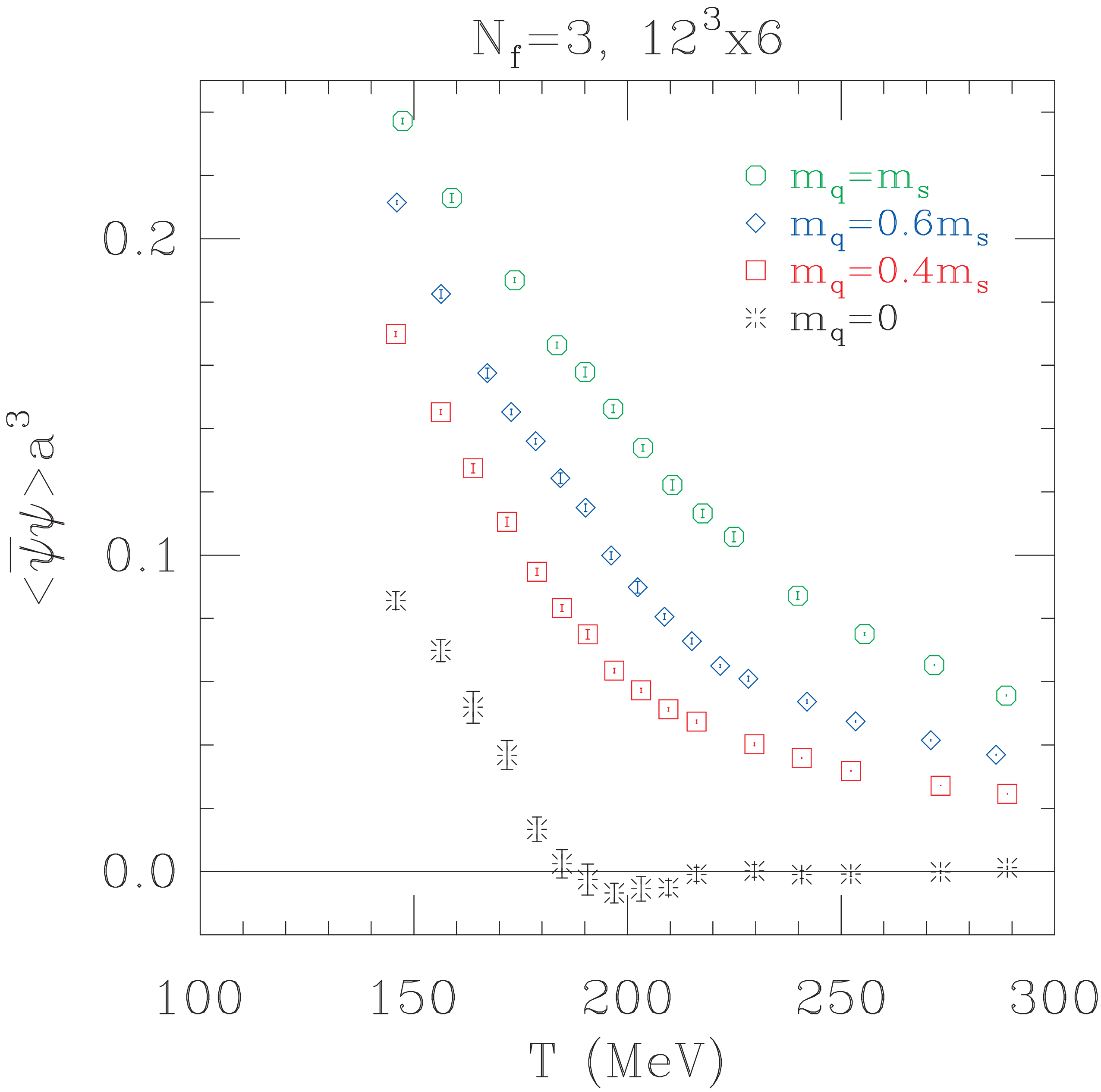

Figure 9: The chiral order parameter, $\bar{\psi}\psi$ on $12^3 \times 6$ lattices. The black bursts are linear extrapolations in the quark mass to $m_q = 0$ for fixed temperature.

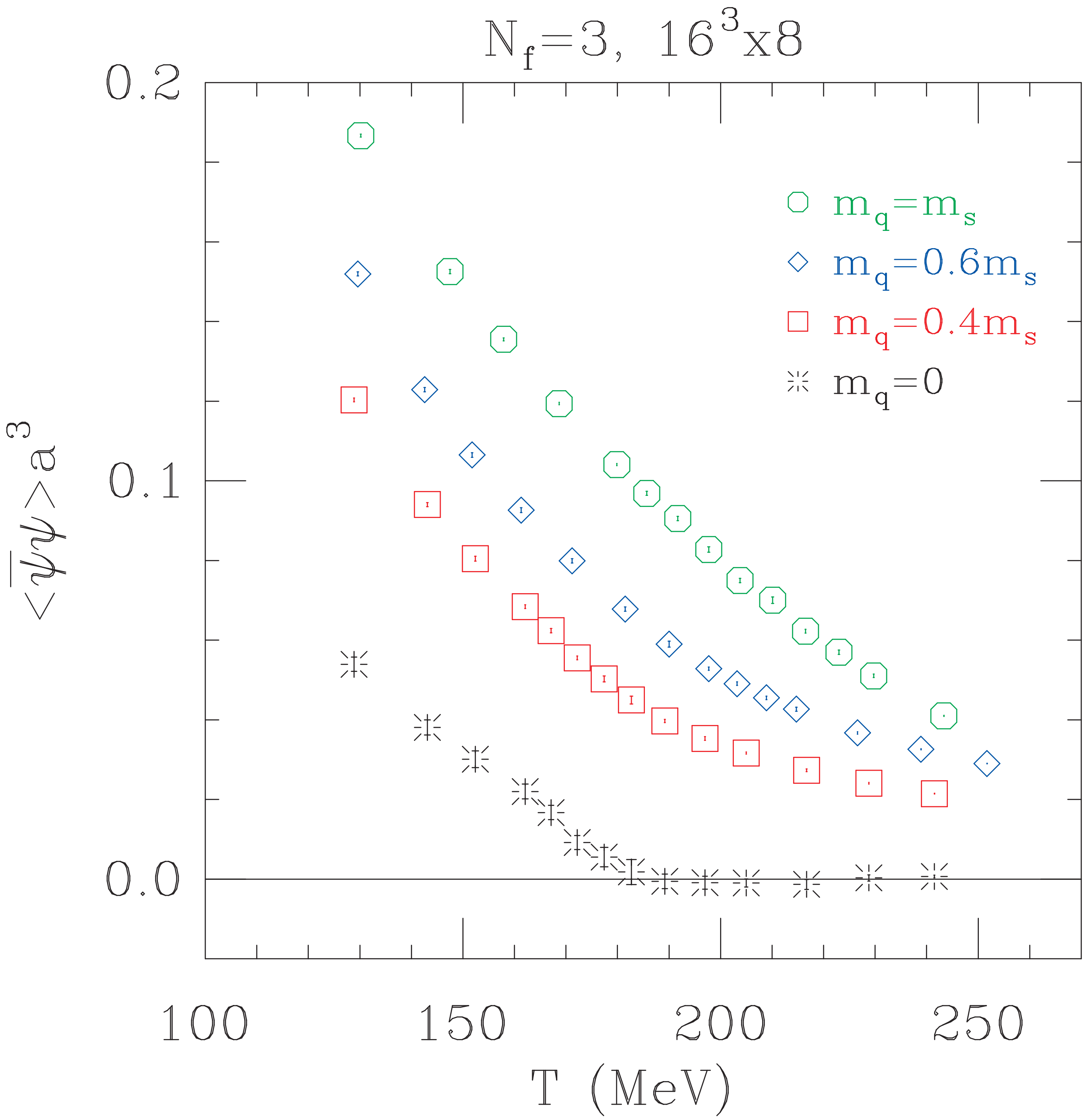

Figure 10: The chiral order parameter, $\bar{\psi}\psi$ on $16^3 \times 8$ lattices. The black bursts are linear extrapolations in the quark mass to $m_q = 0$ for fixed temperature.

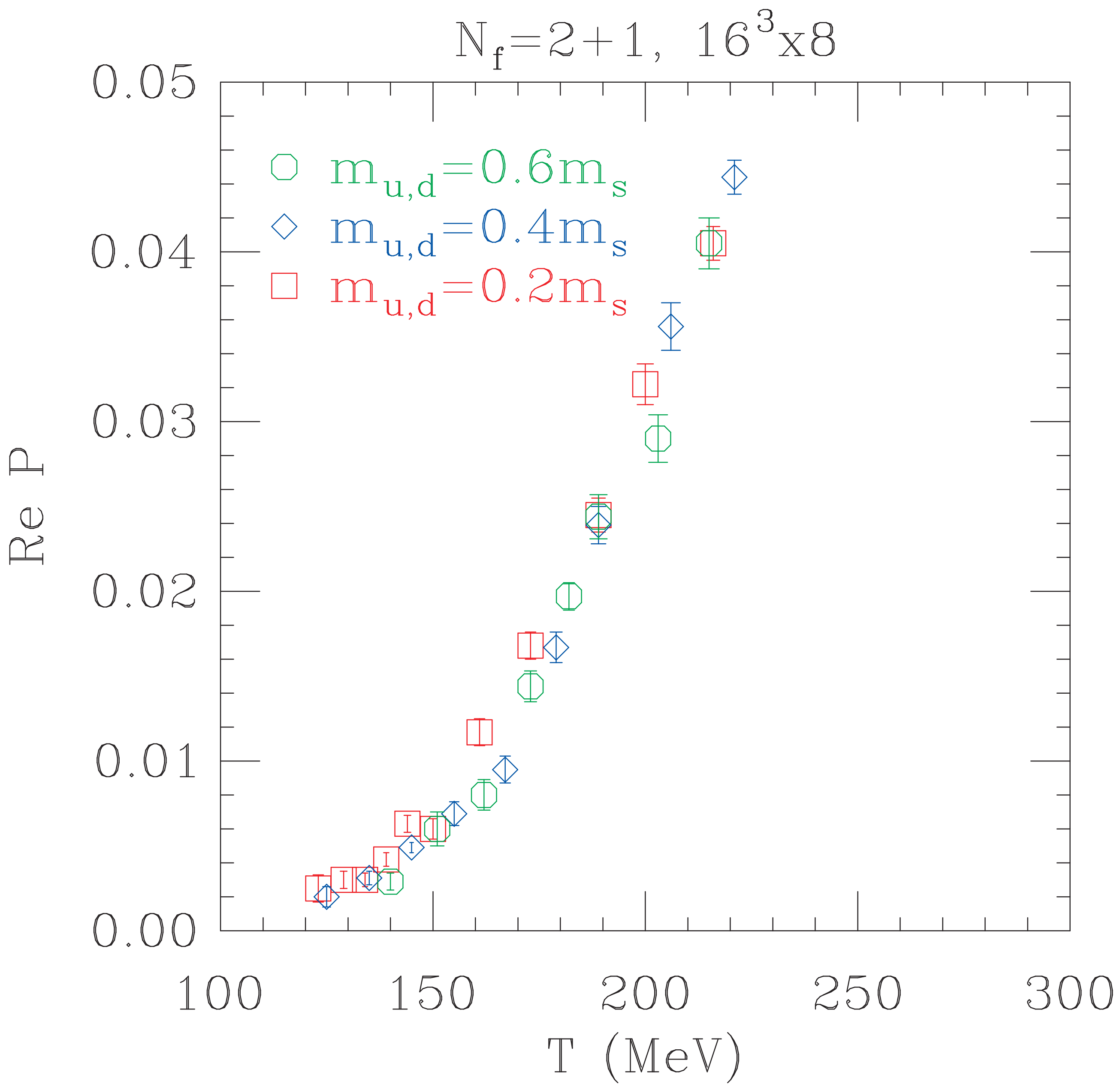

Figure 11: The real part of the Polyakov loop as a function of temperature for two light and one heavy quark on $16^3 \times 8$ lattices. Results are shown for light quark masses $m_{u,d} = 0.6m_s$, $0.4m_s$ and $0.2m_s$. The mass of the heavy quark is fixed at m_s.

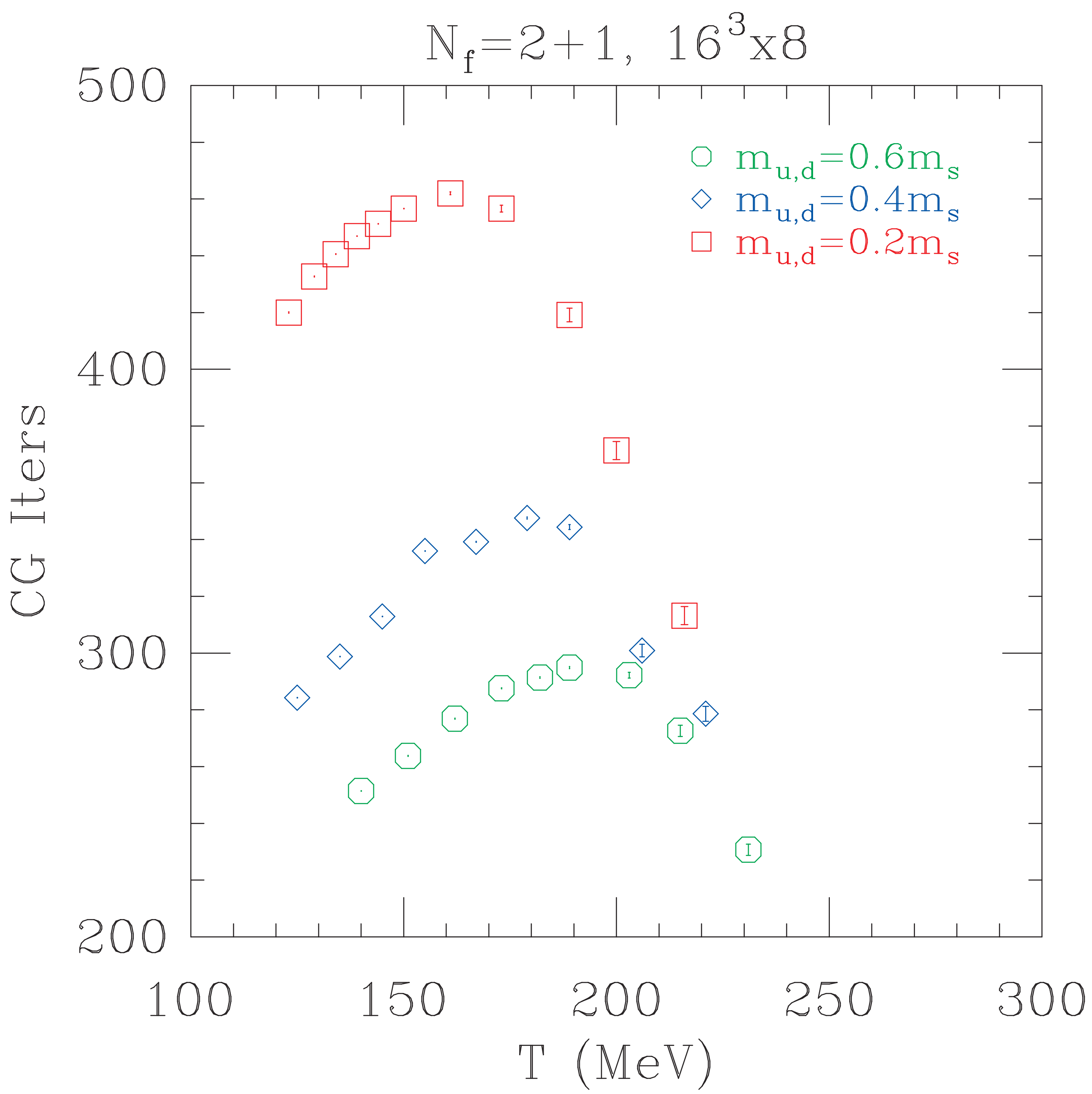

Figure 12: The number of conjugate gradient iterations required for convergence of the inversion of the Dirac operator of light quarks on $16^3 \times 8$ lattices. Results are shown for light quark masses $m_{u,d} = 0.6m_s$, $0.4m_s$ and $0.2m_s$. The mass of the heavy quark is fixed at m_s.

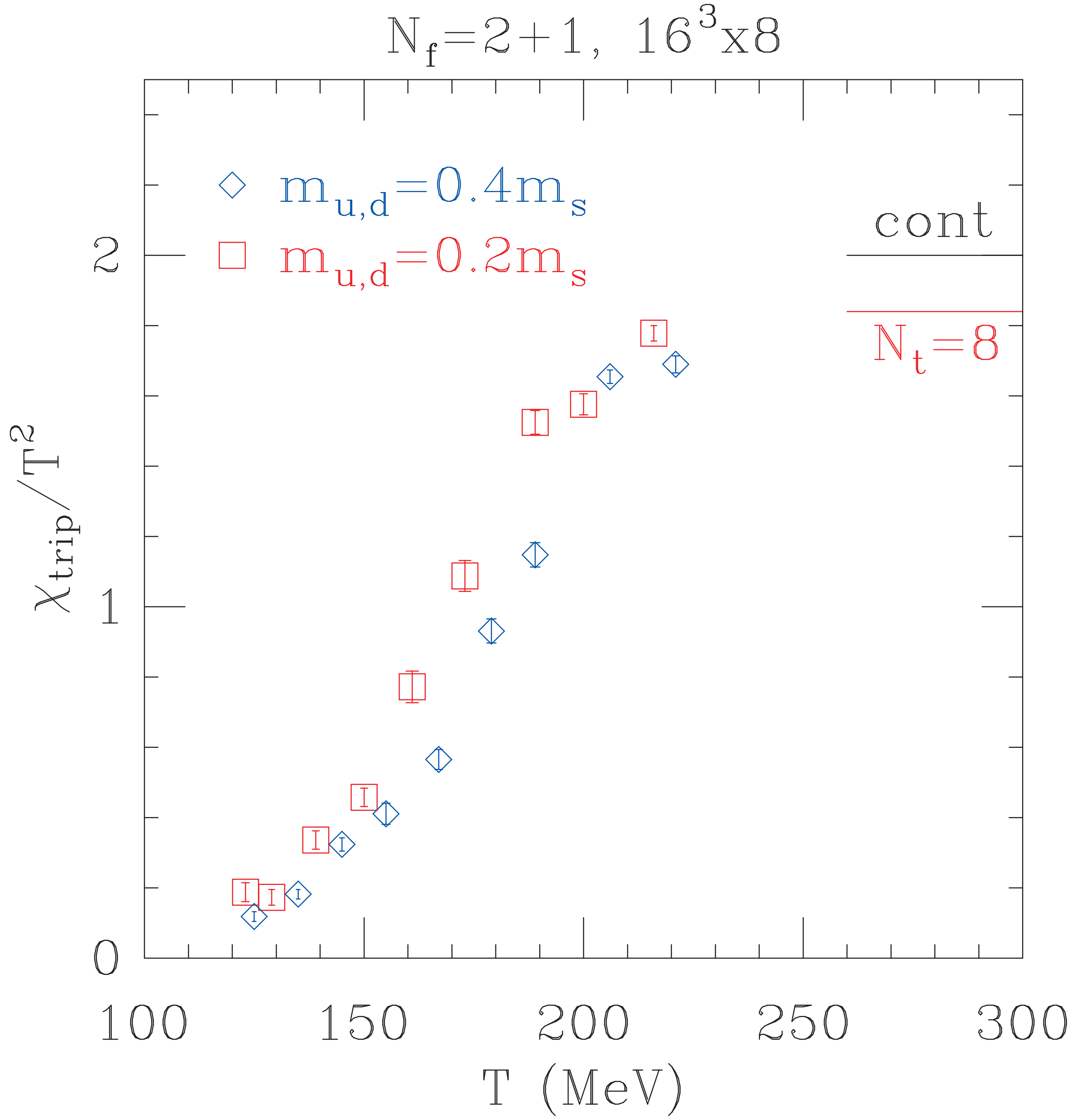

Figure 13: The triplet quark number susceptibility as a function of temperature for two light and one heavy quark on $16^3 \times 8$ lattices. Results are shown for light quark masses $m_{u,d} = 0.6\,m_s$, $0.4\,m_s$ and $0.2\,m_s$. The mass of the heavy quark is fixed at m_s. The black line on the right of the figure indicates the free quark value in the continuum, and the red line the free quark value on a $16^3 \times 8$ lattice.

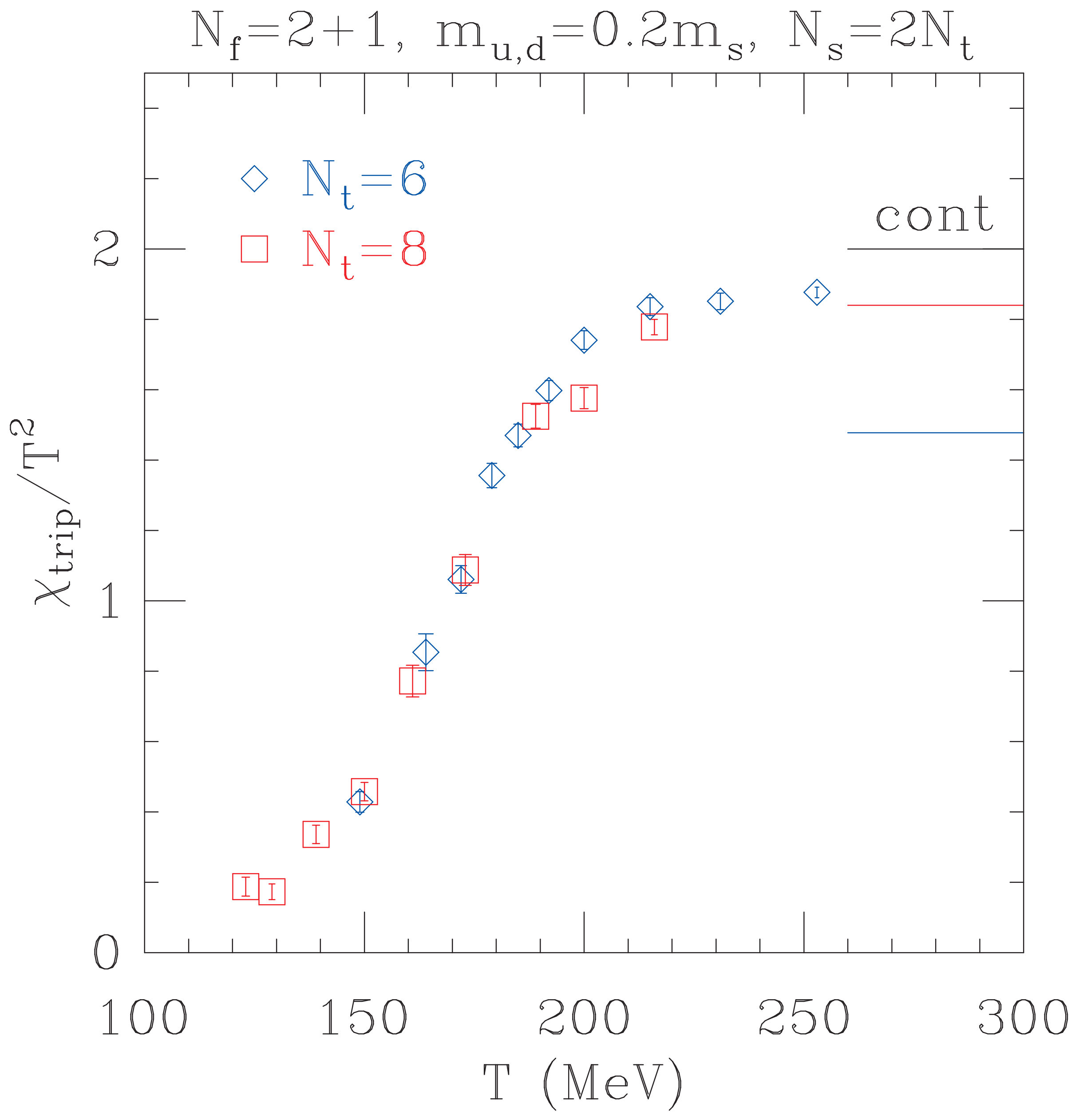

Figure 14: The triplet quark number susceptibility as a function of temperature for two light quarks with mass $0.2m_s$ and one heavy quark with mass m_s. for two light and one heavy quark on $16^3 \times 8$ lattices. Results are shown for $12^3 \times 6$ and $16^3 \times 8$ lattices. The black line on the right of the figure indicates the value for free quarks in the continuum, and the colored lines the value for free quarks on the finite lattices on which the simulations were carried out.

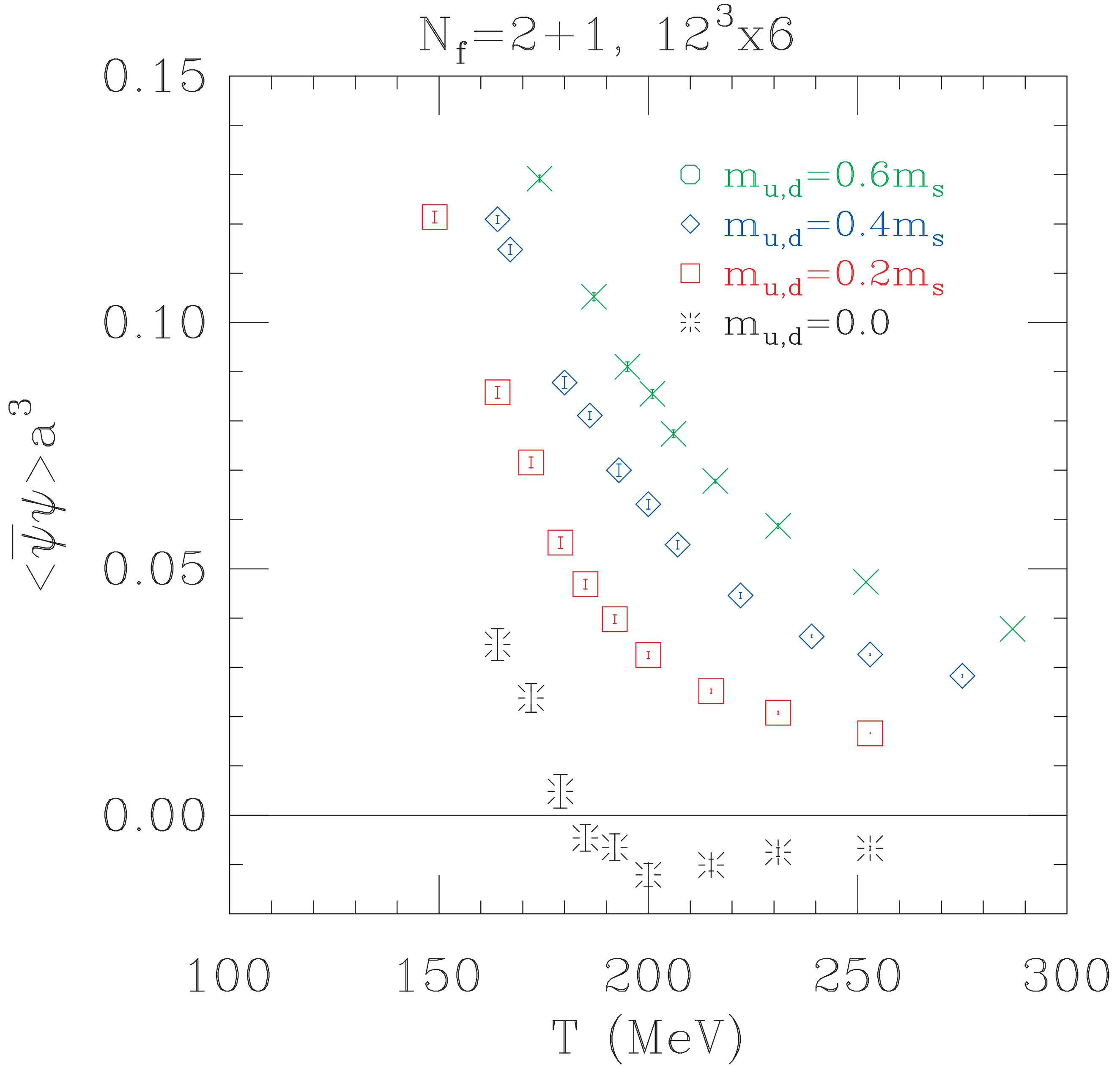

Figure 15: The chiral order parameter, $\bar{\psi}\psi$ on $12^3 \times 6$ lattices. The black bursts are linear extrapolations in the quark mass to $m_q = 0$ for fixed temperature.

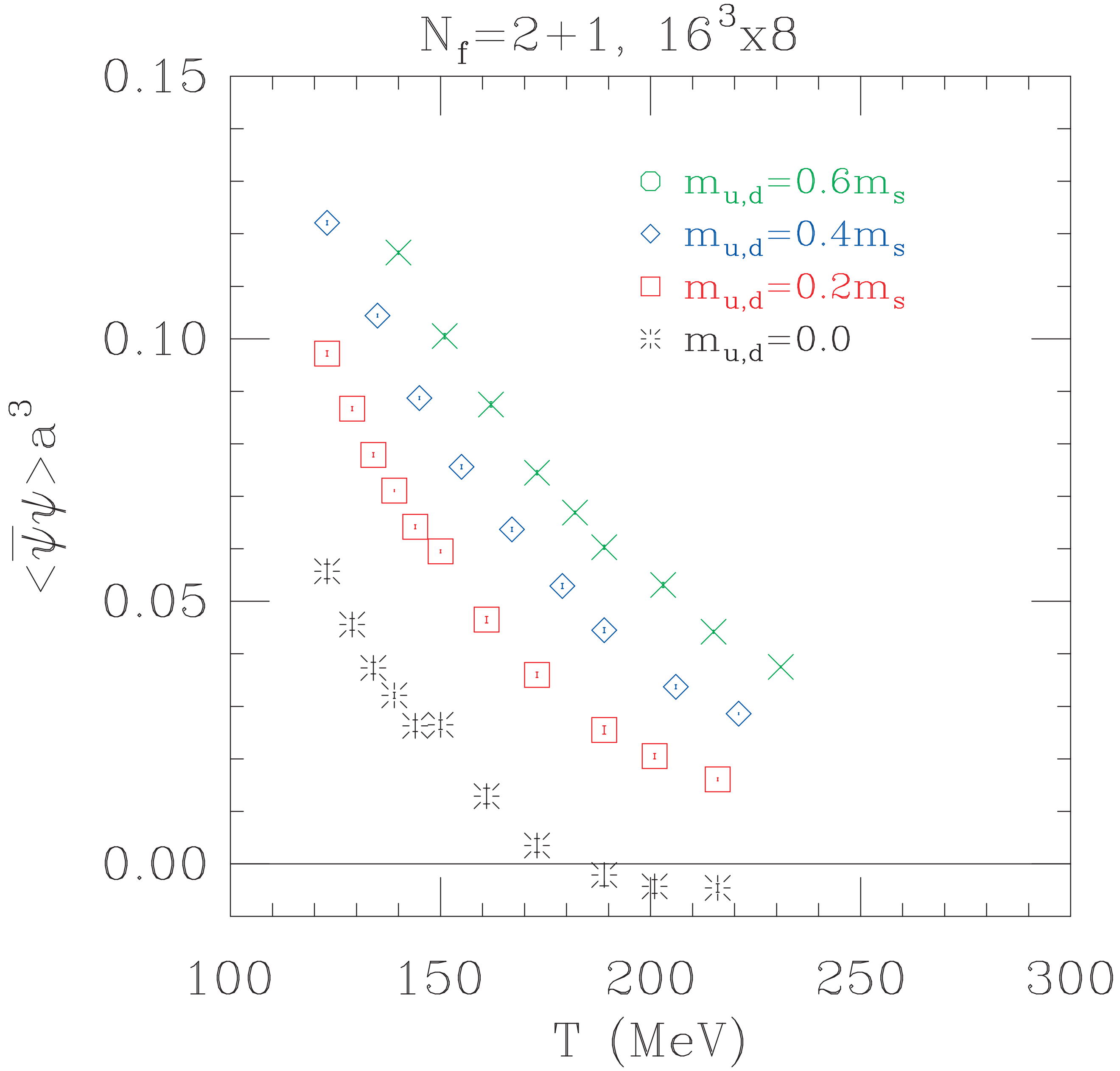

Figure 16: The chiral order parameter, $\bar{\psi}\psi$ on $16^3 \times 8$ lattices. The black bursts are linear extrapolations in the quark mass to $m_q = 0$ for fixed temperature.